

NMR structure note

Solution structure of human dihydrofolate reductase in its complex with trimethoprim and NADPH

Nadezhda V. Kovalevskaya^a, Yegor D. Smurnyy^b, Vladimir I. Polshakov^{a,b}, Berry Birdsall^c, Alan F. Bradbury^c, Tom Frenkiel^d & James Feeney^{c,*}

^aCenter for Drug Chemistry, 119815 Moscow, Russia; ^bCenter for Magnetic Tomography and Spectroscopy, M.V. Lomonosov Moscow State University, 119992 Moscow, Russia; ^cDivision of Molecular Structure, National Institute for Medical Research, The Ridgeway, Mill Hill, London, NW7 1AA, U.K.; ^dMRC Biomedical NMR Centre, National Institute for Medical Research, The Ridgeway, Mill Hill, London, NW7 1AA, U.K.

Received 22 June 2005; Accepted 26 July 2005

Key words: co-operative ligand binding, dihydrofolate reductase, protein structure, protein–ligand interactions, trimethoprim

Abbreviations: DHFR – dihydrofolate reductase; hDHFR – human dihydrofolate reductase; MTX – methotrexate; PDB – Protein Data Bank; TMP – trimethoprim

Biological context

Dihydrofolate reductase (DHFR; EC 1.5.1.3) is a 21.3 kDa (186 amino acids) enzyme that catalyses the NADPH-dependent reduction of folate and 7,8-dihydrofolate to 5,6,7,8-tetrahydrofolate, an important cofactor in the biosynthesis of purines and amino acids. DHFR is an essential enzyme in the cell and is the target for antifolate drugs such as methotrexate, pyrimethamine and trimethoprim that act by inhibiting this enzyme in parasitic or malignant cells (Coulson, 1995). The effectiveness of the antibacterial drug trimethoprim (TMP) results from its binding to the bacterial enzyme being significantly greater than its binding to the vertebrate form of the enzyme (Hitchings, 1989). The specificity of the TMP binding is mainly driven by the strong positive cooperative binding effect between trimethoprim and the cofactor (NADPH) in the binding to bacterial DHFR which is much smaller in the case of human DHFR (Baccanari and Kuyper, 1993). At present there is no satisfactory explanation for the cooperativity in

binding of TMP and NADPH to bacterial DHFR. In order to explore the origins of the specificity and cooperativity it would be useful to compare the structures of the ternary complexes of TMP and NADPH with both the human and bacterial forms of the enzyme. We have previously determined the structure of the ternary complex of bacterial DHFR (*L. casei*) with TMP and NADPH (Polshakov et al., 2002). In the present work, we report the solution structure for the ternary complex of human DHFR (hDHFR). Currently, there are no structures of any complexes of hDHFR in solution in the Protein Data Bank (PDB). Although there are several crystal structures of hDHFR complexed with various ligands in the PDB there are no structures containing the drug trimethoprim. In a previous study, NMR docking was used to position the antitumor compound PT523 into a crystal structure of an analogous complex with hDHFR (Johnson et al., 1997).

Methods and results

Samples of ¹⁵N- and ¹³C,¹⁵N-hDHFR were expressed in *E. coli* strain Rosetta (Novagen) grown

*To whom correspondence should be addressed. E-mail: jfeeney@nimr.mrc.ac.uk

on M9 minimal medium containing 99% ^{13}C -glucose (Cambridge Isotope Laboratories) and/or 99% ^{15}N -ammonium sulphate as the sole carbon and nitrogen sources, respectively. Unlabelled hDHFR was prepared in a similar manner using non-labelled materials. Purification of the protein was conducted as described earlier (Prendergast et al., 1988) with some minor changes.

The NMR samples were approximately 1 mM solutions of the equimolar complex hDHFR.TMP.NADPH (ligands from Sigma) prepared in either 100% D_2O or 95% $\text{H}_2\text{O}/5\%$ D_2O and 50 mM potassium phosphate, 100 mM KCl at pH 6.5.

All spectra were acquired at 15 °C on Varian UNITY 600 MHz and Varian INOVA 600 and 800 MHz spectrometers equipped with triple resonance z-gradient probes. Spectra were processed by VNMR and NMRPipe (Delaglio et al., 1995), and analysed using XEASY (Bartels et al., 1995) and SPARKY (Goddard, (T.D. Goddard and D.F. Kneller, SPARKY 3, University of California, San Francisco, U.S.A.)). Sequential assignments for the protein backbone were obtained using $[\text{H},^{15}\text{N}]$ HSQC (Figure 1aS in supplementary material), HNCA, HN(CO)CA, HNCOC, HNCACB, CBCA(CO)NH and HBHA(CO)NH spectra. Aliphatic side-chain resonances were derived from 3D HCCH-TOCSY, HNHB, $[\text{H},^{15}\text{N}]$ NOESY-HSQC, $[\text{H},^{13}\text{C}]$ NOESY-HSQC, $[\text{H},^{13}\text{C}]$ HMQC-NOESY, 2D $[\text{H},^{13}\text{C}]$ HSQC and DQF-COSY spectra. The signals from aromatic ring protons and

carbons were assigned using 2D $[\text{H},^{13}\text{C}]$ HSQC, DQF-COSY and 3D $[\text{H},^{13}\text{C}]$ HMQC-NOESY spectra. Resonance assignments of the ligand signals (TMP and NADPH) were extracted from an analysis of 2D ^{13}C - and ^{15}N -filtered NOESY (Figure 1bS in supplementary material) and 2D NOESY spectra. The NMR experimental methods were similar to those used earlier (Polshakov et al., 1999).

More than 98% of all possible protein signals including those from virtually all of the non-exchangeable protons in bound TMP and NADPH were assigned. The ^1H , ^{15}N and ^{13}C chemical shifts have been deposited in the BioMagRes Bank database (<http://www.bmrb.wisc.edu>) under the Accession No. BMRB-5981. Partial assignments for the complex with methotrexate had been reported earlier by Stockman et al. (1992).

Protein-protein NOEs were assigned in 3D $[\text{H},^{15}\text{N}]$ and $[\text{H},^{13}\text{C}]$ NOESY-HSQC, $[\text{H},^{13}\text{C}]$ HMQC-NOESY and 2D NOESY experiments recorded at 15 °C with 50 ms mixing times. Ligand-ligand and protein-ligand NOEs were identified in 2D ^{15}N - and ^{13}C -filtered NOESY experiments (Figure 1bS in supplementary material). Torsion angle restraints were determined from analysis of chemical shift values using the TALOS program (Cornilescu et al., 1999). Determinations of TMP torsion angle restraints and protein stereospecific assignments were carried out using the program AngleSearch (Polshakov et al., 1995).

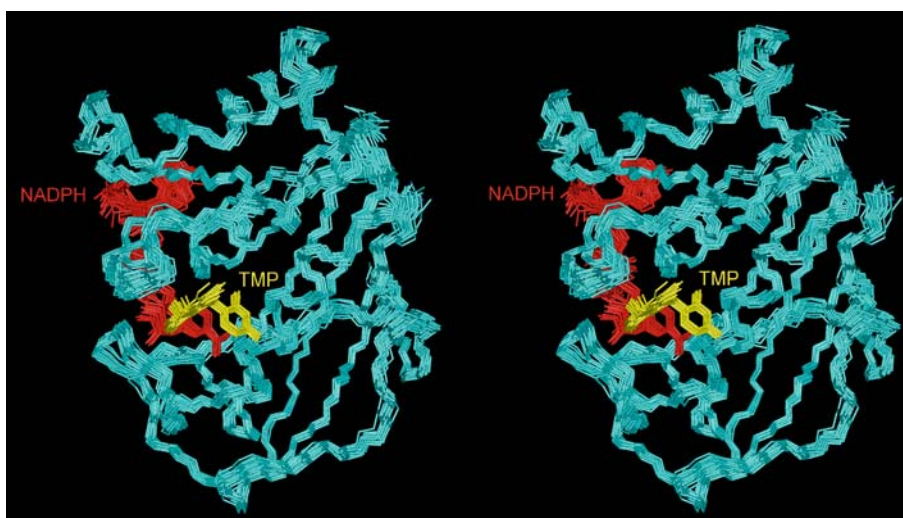


Figure 1. Stereoview of a superposition over the backbone atoms (N, C α and C) of residues 1–186 of the final 25 structures of the hDHFR.TMP.NADPH complex. The ligands TMP and NADPH are coloured yellow and red, respectively. The superposition was made onto the backbone atoms of the representative structure, S_{rep} .

Distance constraints were calibrated and structures calculated using the ARIA 2.0 (Habeck et al., 2004) and CNS 1.1 (Brünger et al., 1998) programs, essentially using the default setting from ARIA. 3565 NOE restraints, 326 torsion angles, 139 hydrogen bonds and 258 ^1H chemical shifts for $\text{H}\alpha$ and methyl groups were used to determine the 3D solution structure of the complex using the CNS simulated annealing protocol.

The quality of the final ensemble of structures was assessed with PROCHECK NMR (Laskowski et al., 1996) (see supplementary material Figures 2S, 3S and 4S). The final ensemble contained 25 structures with the quality defined in Table 1 (supplementary materials) and Figures 1 and 5S (the latter in supplementary materials). The coordinates have been deposited into the Protein Data Bank (PDB) under Accession No. 1YHO.

Discussion and conclusions

Figure 1 shows the ensemble of NMR structures for the ternary complex hDHFR.TMP.NADPH. The overall fold is similar to that found in the crystal structures of its various complexes. Superposition of the representative solution structure of hDHFR.TMP.NADPH onto the X-ray structure of the complex of hDHFR with NADPH and a pyridopyrimidine antifolate (1PD8, Cody et al., 2003) gives 1.26 Å RMSD for the protein backbone atoms.

Conformation of bound TMP and its binding site

The structure of the bound TMP is very well defined in the family of 25 NMR structures (see Figure 5S in supplementary material). The values of the torsion angles τ_1 and τ_2 are $206.67^\circ \pm 2.45^\circ$ and $82.11^\circ \pm 4.93^\circ$, respectively (where τ_1 is defined as C4–C5–C7–C11 and τ_2 as C5–C7–C11–C12). This conformation is found to be rather similar to that in the complex of lcdHFR.TMP.NADPH: $195.57^\circ \pm 7.72^\circ$ and $73.99^\circ \pm 7.51^\circ$ for τ_1 and τ_2 , respectively (Polshakov et al., 2002).

Trimethoprim occupies the substrate binding site as seen from comparison with the crystal structure of the complex of hDHFR with folate (Davies et al., 1990). The protonated N1 atom of TMP is in close contact with OE1 of Glu30 (2.82 Å) (see Figure 2a) which is in agreement with

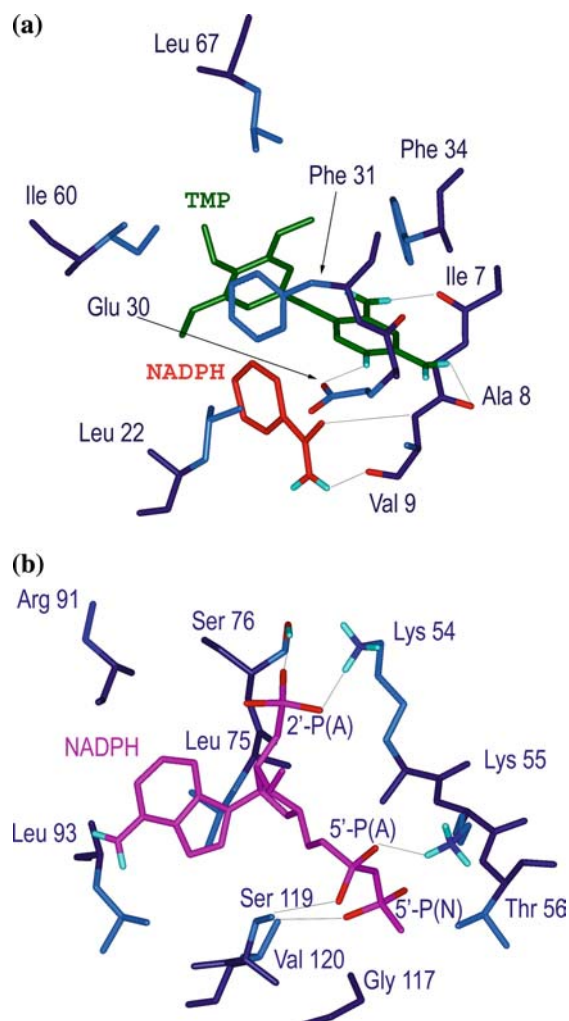


Figure 2. Interactions between hDHFR and the ligands for: (a) TMP (green) and the reduced nicotinamide ring of NADPH (red) (b) the adenosine moiety and pyrophosphate backbone of NADPH (mauve). Hydrogen bonds are indicated by grey lines.

previous findings (Roberts et al., 1981; Birdsall et al., 1989) that TMP is protonated at N1 and involved in electrostatic interactions with a carboxylate group in the protein.

Conformation of bound NADPH and its binding site

NADPH binds to hDHFR in an extended conformation over the surface of the protein (see Figure 1). The structure of the bound coenzyme is well defined (see Figure 5S) with an RMSD value of 1.26 ± 0.35 Å. The nicotinamide carboxamide group is in the *trans*-conformation and forms

hydrogen bonds to Ala9 (carbonyl group), Ile16 (carbonyl group) and Val9 (NH group) (see Figure 2a). The structure of the pyrophosphate group is less well defined due to the absence of direct NOE effects. However, the analysis of the final structure reveals the network of hydrogen bonds from oxygen atoms of pyrophosphate to Ser119, Val120 and Lys55. The adenine ring lies in a hydrophobic cleft formed by Leu75, Leu93, Arg91 and Val120 (see Figure 2b).

The conformation of bound NADPH and its protein interactions in solution are in good agreement with results reported for crystal structures of human DHFR complexes containing NADPH (PDB codes 1KMV and 1KMS, Klon et al., 2002). The most noticeable differences (~ 1 Å displacement and $\sim 35^\circ$ change in orientation) are seen for the nicotinamide ring between conformations of coenzyme in the crystal (1KMV) and solution hDHFR structures.

Interactions between ligands

Parts of bound TMP and NADPH are in close proximity to each other and the contact region between them is shown in Figures 1 and 2a and 5S (in supplementary materials). The protein interface between ligands involves Trp24 and Lys22 residues which hydrophobically interact both with the TMP trimethoxy ring and the NADPH nicotinamide ring. The closest contact between the ligands is between the C4 position of nicotinamide ring and methylene C7 of TMP. This internuclear distance is very similar in the two complexes measuring between 3.24 and 3.26 Å. It thus seems likely that the origin of the differences in cooperative ligand binding is not caused by differences in the direct interactions of the two ligands with each other but rather by differences in the ligand interactions with the proteins.

Electronic supplementary material is available at <http://dx.doi.org/10.1007/s10858-005-1475-z>.

Acknowledgements

The NMR measurements were carried out at the MRC Biomedical NMR Centre, Mill Hill. We thank Dr D. Stuber (Hoffman-La Roche) for providing the pB-E1/RBSII,SphI-hDHFR plas-

mid construct, Dr G. Kelly for help in setting up the NMR experiments and Drs A. Gargaro and U. Wollborn for their valuable help in the preliminary stages of the NMR spectral analysis. This research is supported by the Medical Research Council, U.K., a Wellcome Trust Collaborative Research Initiative Grant 060140, and a grant from the Russian Foundation for Basic Research. VIP is an International Scholar of the Howard Hughes Medical Institute.

References

- Baccanari, D.P. and Kuyper, L.F. (1993) *J. Chemother.*, **5**, 393–399.
- Bartels, Ch., Xia, T.-H., Billeter, M., Güntert, P. and Wüthrich, K. (1995) *J. Biomol. NMR*, **5**, 1–10.
- Birdsall, B., Andrews, J., Ostler, G., Tendler, S.J.B., Feeney, J., Roberts, G.C.K., Davies, R.W. and Cheung, H.T.A. (1989) *Biochemistry*, **28**, 1353–1362.
- Brünger, A.T., Adams, P.D., Clore, G.M., DeLano, W.L., Gros, P., Grosse-Kunstleve, R.W., Jiang, J.S., Kuszewski, J., Nilges, M., Pannu, N.S., Read, R.J., Rice, L.M., Simonson, T. and Warren, G.L. (1998) *Acta Crystallogr. D Biol. Crystallogr.*, **54**, 905–921.
- Cody, V., Luft, J.R., Pangborn, W. and Gangjee, A. (2003) *Acta Crystallogr. Sect. D*, **59**, 1603–1609.
- Cornilescu, G., Delaglio, F. and Bax, A. (1999) *J. Biomol. NMR*, **13**, 289–302.
- Coulson, C.J. (1995) *Molecular Mechanisms of Drug Action* Taylor & Francis, London.
- Davies, J.F., Delcamp, T.J., Prendergast, N.J., Ashford, V.A., Freisheim, J.H. and Kraut, J. (1990) *Biochemistry*, **29**, 9467–9479.
- Delaglio, F., Grzesiek, S., Vuister, G.W., Zhu, G., Pfeifer, J. and Bax, A. (1995) *J. Biomol. NMR*, **6**, 277–293.
- Habeck, M., Rieping, W., Linge, J.P. and Nilges, M. (2004) *Methods Mol. Biol.*, **278**, 379–402.
- Hitchings, G.H. (1989) *Angew. Chem. Int. Ed.*, **28**, 879–885.
- Johnson, J.M., Meiering, E.M., Wright, J.E., Pardo, J., Rosowsky, A. and Wagner, G. (1997) *Biochemistry*, **36**, 4399–4411.
- Klon, A.E., Heroux, A., Ross, L.J., Pathak, V., Johnson, C.A., Piper, J.R. and Borhani, D.W. (2002) *J. Mol. Biol.*, **320**, 677–693.
- Laskowski, R.A., Rullmann, J.A.C., MacArthur, M.W., Kaptein, R. and Thornton, J.M. (1996) *J. Biomol. NMR*, **8**, 477–486.
- Polshakov, V.I., Frenkiel, T.A., Birdsall, B., Soteriou, A. and Feeney, J. (1995) *J. Magn. Reson. B*, **108**, 31–43.
- Polshakov, V.I., Birdsall, B. and Feeney, J. (1999) *Biochemistry*, **38**, 15962–15969.
- Polshakov, V.I., Smirnov, E.G., Birdsall, B., Kelly, G. and Feeney, J. (2002) *J. Biomol. NMR*, **24**, 67–70.
- Prendergast, N.J., Delcamp, T.J., Smith, P.L. and Freisheim, J.H. (1988) *Biochemistry*, **27**, 3664–3671.
- Roberts, G.C.K., Feeney, J., Burgen, A.S.V. and Daluge, S. (1981) *FEBS Lett.*, **131**, 85–88.
- Stockman, B.J., Nirmala, N.R., Wagner, G., Delcamp, T.J., DeYarman, M.T. and Freisheim, J.H. (1992) *Biochemistry*, **31**, 218–229.